Hydrogen Separation Membranes based on Dense Ceramic Composites in the $La_{27}W_5O_{55.5}$–$LaCrO_3$ System

Jonathan. M. Polfus[a], Wen Xing, Marie-Laure Fontaine, Christelle Denonville, Partow P. Henriksen, Rune Bredesen

[a]*SINTEF Materials and Chemistry, Sector for Sustainable Energy Technology, Forskningsveien 1, NO-0314 Oslo, Norway*

*Contact email: jonathan.polfus@sintef.no

Abstract

Some compositions of ceramic hydrogen permeable membranes are promising for integration in high temperature processes such as steam methane reforming due to their high chemical stability in large chemical gradients and CO_2 containing atmospheres. In the present work, we investigate the hydrogen permeability of densely sintered ceramic composites (cercer) of two mixed ionic-electronic conductors: $La_{27}W_{3.5}Mo_{1.5}O_{55.5-\delta}$ (LWM) containing 30, 40 and 50 wt% $La_{0.87}Sr_{0.13}CrO_{3-\delta}$ (LSC). Hydrogen permeation was characterized as a function of temperature, feed side hydrogen partial pressure (0.1-0.9 bar) with wet and dry sweep gas. In order to assess potentially limiting surface kinetics, measurements were also carried out after applying a catalytic Pt-coating to the feed and sweep side surfaces. The apparent hydrogen permeability, with contribution from both H_2 permeation and water splitting on the sweep side, was highest for LWM70-LSC30 with both wet and dry sweep gas. The Pt-coating further enhances the apparent H_2 permeability, particularly at lower temperatures. The apparent H_2 permeability at 700 °C in wet 50% H_2 was 1.1×10^{-3} mL min^{-1} cm^{-1} with wet sweep gas, which is higher than for the pure LWM material. The present work demonstrates that designing dual-phase ceramic composites of mixed ionic-electronic conductors is a promising strategy for enhancing the ambipolar conductivity and gas permeability of dense ceramic membranes.

Keywords*:* hydrogen separation; dense ceramic membrane; ceramic-ceramic composite; lanthanum tungstate; lanthanum chromite

1. Introduction

Technology utilizing hydrogen permeable membranes that are stable at high temperatures is promising for application in a range of processes including power generation with pre-combustion CO_2 capture and production of hydrogen and other valuable chemicals from various feedstock in membrane reactors.[1–6] In contrast to other types of inorganic hydrogen selective membranes, the dense ceramic membranes are stable at temperatures above 700 °C in conditions relevant for these applications.[7,8] However, increased hydrogen flux of these membranes is essential for industrial deployment.

Hydrogen permeation in mixed protonic and electronic conducting ceramics is driven by a hydrogen chemical potential gradient across the membrane and proceeds according to ambipolar transport of protons and electronic charge carriers. Hydrogen permeability is thereby limited by the slowest of these species as described by the ambipolar conductivity of the material. Two main strategies are applied for enhancing transport of the less conducting species, which for chemically stable proton conductors often is electronic: 1) dissolution of multivalent dopants such as Ru, Eu, and Mo, as demonstrated for $BaCeO_{3-\delta}$,[9] $SrCeO_{3-\delta}$[10] and $La_{27}W_5O_{55.5-\delta}$[11,12], respectively; 2) use of a percolating metal phase of for instance Ni or Pd in a cermet composite as demonstrated for $BaCeO_{3-\delta}$, $BaZrO_{3-\delta}$ and $CeO_{2-\delta}$ based ceramics.[13–17] Unemoto et al.[18] employed a proton conducting and an electron conducting oxide in their investigation of $SrZrO_{3-\delta}$–$SrFeO_{3-\delta}$ ceramic-ceramic composites (cercer), which showed considerable hydrogen permeability albeit lower than what was estimated from ambipolar conductivities. Xing et al.[19] recently reported appreciable hydrogen permeation through cercer membranes of proton conducting Ca-doped $LaNbO_{4-\delta}$ and electronically conducting $LaNb_3O_{9-\delta}$, with ambipolar conductivities limited by electronic and protonic transport for 10 and 30 vol% $LaNb_3O_{9-\delta}$, respectively. Fish et at.[20] are currently pursuing a similar approach through their investigation of Y- and Ce-doped $BaZrO_{3-\delta}$ and Nd-doped $SrTiO_{3-\delta}$ cercer.

In the present work, we investigate the hydrogen permeation characteristics of cercer membranes comprising two mixed ionic and electronic conductors, $La_{27}W_{3.5}Mo_{1.5}O_{55.5-\delta}$ and $La_{0.87}Sr_{0.13}CrO_{3-\delta}$, hereafter referred to as LWM and LSC, respectively. This composite material system for hydrogen membranes has recently been developed and characterized by Universidad Politécnica de Valencia (Spain) and Protia AS (Norway) and exhibits state-of-the-art H_2 permeation for dense ceramic membranes.[21,22] As described below, the ambipolar conductivity of these materials is limited by ionic and electronic transport in different temperature regimes, and the prospect of a cercer membrane attributing the complementary characteristics of both materials is enticing. Furthermore, as recently elucidated in detail for LSC membranes,[23,24] splitting of water under wet sweep gas conditions by oxide ion transport through the membrane, driven by an oxygen chemical potential gradient, will yield additional H_2 in the permeate. It may be beneficial to utilize H_2 from both permeation and water splitting in a process scheme.[23]

Lanthanide tungstate based materials with nominal stoichiometries close to $3(Ln_2O_3)\cdot(WO_3)$ have attracted much attention due to their high and predominating proton conductivity in wet atmospheres below approx. 750 °C and mixed protonic electronic conductivity at higher temperatures.[25–33] Lanthanum tungstate is found to be single phase for La/W ratios in the range 5.3-5.7,[29] owing to a stabilizing effect of substituting W on La sites within the fluorite related structure.[34] The formula unit may therefore be written $La_{28-x}W_{4+x}O_{54+3x/2}v_{2-3x/2-\delta}$, where x quantifies W substituted on La sites and v denotes inherently vacant oxygen sites.[35] Vøllestad et al.[12] recently characterized the hydrogen permeability in $La_{27}W_{3.5}Mo_{1.5}O_{55.5-\delta}$, where the Mo-substitution substantially increases n-type electronic conductivity under reducing conditions without significantly altering the protonic conductivity.[11]

Lanthanum chromite, $LaCrO_{3-\delta}$, is a widely studied refractory perovskite oxide in particular due to its chemical stability over a wide range of p_{O_2} and significant p-type electronic conductivity from oxidizing to moderately reducing conditions when acceptor doped with, e.g., Ca or Sr on La site.[36,37] The acceptor doped material exhibits appreciable O_2 permeability due oxygen vacancies partly charge compensating the acceptor,[38,39] and it has been investigated as a hydrogen permeable membrane due to dissolution of protons in wet hydrogen containing atmospheres.[23,40] Vigen et al.[24] have recently provided a detailed characterization of the hydrogen permeability of $La_{0.87}Sr_{0.13}CrO_{3-\delta}$ involving a significant increase in H_2 permeability upon coating the surface with a porous Pt layer, indicating limiting surface kinetics for uncoated samples. Nevertheless, the applicability of $LaCrO_{3-\delta}$ based materials is challenged by their poor sinterability, and significant efforts have been devoted to mitigate this problem including use of sintering aids and reducing atmospheres.[41–43] Further details of the H_2 permeation and water splitting characteristics reported for LWM and LSC based membranes will be discussed in conjunction with the results in the present work.

2. Experimental

2.1 Synthesis and characterization

Powders of $La_{27}W_{3.5}Mo_{1.5}O_{55.5-\delta}$ (LWM) and $La_{0.87}Sr_{0.13}CrO_{3-\delta}$ (LSC) were synthesized by spray-pyrolysis (Marion Technologies and Praxair, respectively). The particle size distribution of the powder was determined by laser granulometry using a Malvern Mastersizer 2000 apparatus and the specific surface area was determined from N_2 adsorption-desorption using a Quantachrome Monosorb apparatus.

Mixtures of LWM with 30, 40 and 50 wt% LSC were homogenized by ball milling overnight in a plastic container using zirconia balls. These mixtures correspond to 29.3, 39.1 and 48.9 vol% LSC, respectively, with nominal densities of 6.45 and 6.59 g cm^{-3} for LWM and LSC, respectively. Symmetric disc samples (∅ = 21 mm) were prepared by uniaxial cold pressing at 85 MPa and the samples were sintered at 1475 °C in ambient air for 6 h with heating and cooling rates of 240 °C h^{-1}. The samples are denoted according to their LWM and LSC contents in wt%, i.e., LWM70-LSC30, LWM60-LSC40 and LWM50-LSC50, and the sample thicknesses were 1.43, 1.13 and 1.21 mm, respectively.

The phase purity of both powders and the sintered cercer materials was determined by X-ray diffraction using a Panalytical Empyrean diffractometer with Cu Kα radiation and PIXcel^{3D} detector. The diffraction data were analyzed using the Le Bail method as implemented in the TOPAS software by Bruker. The microstructure of the sintered specimens was studied with a FEI Quanta 200 F scanning electron microscope (SEM).

2.2 Hydrogen permeation measurements

The disc samples were polished gradually to a roughness of 3 μm with SiC grinding paper and subsequently using diamond paste. Slightly isostatically pressed and similarly polished gold O-ring gaskets (made by welding gold wire of ∅ = 1 mm) were used for sealing the samples (∅ ≈ 16 mm) to an alumina support tube (∅ = 13 mm) in a ProboStat measurement cell (NorECs, Norway). An alumina spring load assembly was used to provide a force of 45 N on the sample against the gold gasket and alumina support tube.

The measurement cell provides a gas tight environment and mass flow controllers were utilized to supply H_2/N_2/He feed gas mixtures and argon sweep gas at 50 and 25 mL min^{-1}, respectively. Wet feed and sweep gas mixtures were obtained by bubbling through a saturated KBr solution, yielding a water content of 2.5 % H_2O. The concentrations of H_2 permeate and He leakage were measured by a Varian CP-4900 gas chromatograph (GC).

An S-type thermocouple was placed in the vicinity of the gold O-ring inside the measurement cell, which was inserted into a vertical tube furnace. A successful seal, as

determined by a He leakage below the background He level in the GC, i.e., approx. 5 ppm, was usually obtained by heating to 950 °C. Hydrogen permeation fluxes were measured as function of hydrogen partial pressure in the range 0.1-0.9 bar at temperatures between 600-900 °C. The He feed was kept constant at 5 mL min^{-1} and the H_2/N_2 ratio was varied. In order to investigate the possibility of limiting surface kinetics, permeation measurements were also carried out after applying platinum ink (Engelhard A-3788) to the feed and sweep side of the specimen and heating in air. For dense ceramic membranes, the H_2 permeability, J_{H_2}, is taken as the thickness corrected H_2 flux at given feed and sweep side conditions with units mL min^{-1} cm^{-1}.

3. Results

3.1 Sample preparation and characterization

As determined by laser granulometry and N_2 adsorption-desorption measurements, the powders of LWM and LSC are characterized by a median particle size of 2.14 and 0.075 μm, respectively, and a surface area of 2.9 g m^{-2} for LWM and 2.3 g m^{-2} for LSC. Figure **1** shows an X-ray diffractogram of the LWM50-LSC50 powders before sintering fitted to LWM ($F\bar{4}3m$, a=11.180 Å) and two LSC phases ($Pbnm$, a=5.491, b=5.462, c=7.767 Å) and ($R\bar{3}c$, a=5.505, c=13.295 Å). The LWM lattice parameter (nominally 30 mol% Mo) is slightly smaller than that reported for 20 and 40 mol% Mo-doped and La-deficient LWM, 11.188 and 11.191 Å, respectively.[11] The cell volumes of the LSC phases, 233.0 and 348.9 $Å^3$ for $Pbnm$ and $R\bar{3}c$, respectively, are similar to those reported for 12 mol% Sr-doped LSC, 234.0 and 350.0 $Å^3$.[41]

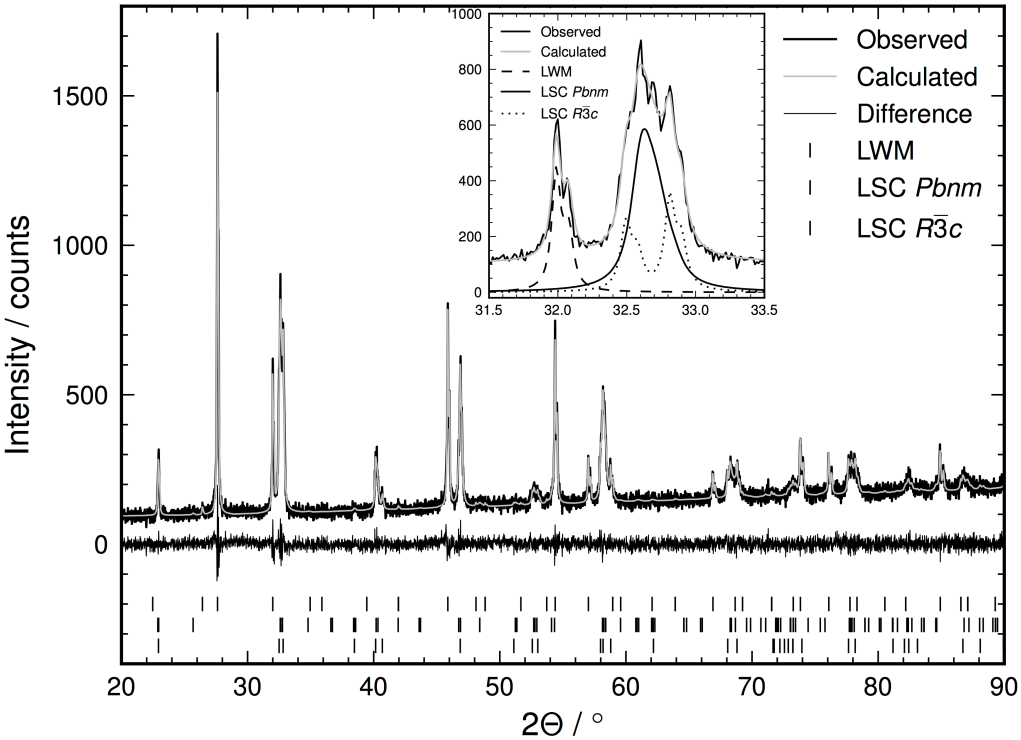

Figure 1: X-ray diffractogram of the LWM50-LSC50 powders with Le Bail fitting for LWM and two LSC phases. The inset shows the individual calculated peaks, substantiating the presence of both LSC phases.

The relative densities of the sintered specimens was estimated to be >99 % based on theoretical densities determined from XRD lattice parameters, nominal stoichiometry and composite ratios. SEM surface micrographs of the sintered specimens (Figure **2**) show a

homogeneous mixture of LWM and LSC in the cercer membranes. The LWM grain size (lighter phase), approx. 5 µm, is slightly larger than that of the LSC grains, approx. 1-3 µm. This difference can be related to the initial difference in particle size of the powders, and may be further attributed to the lower sinterability of LSC materials.

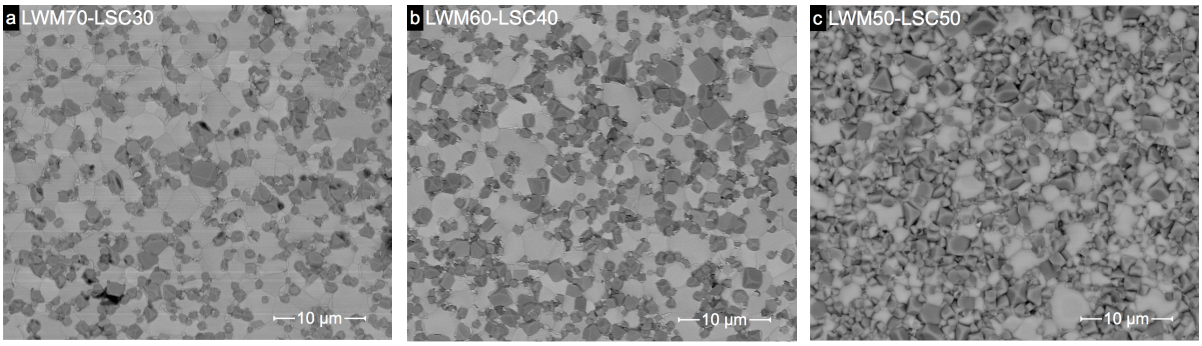

Figure 2: SEM surface micrographs of the sintered specimens obtained with the backscattered detector showing homogeneous mixtures of LWM (lighter phase) and LSC (darker phase) for LWM70-LSC30 (a), LWM60-LSC40 (b) and LWM50-LSC50 (c).

3.2 H_2 permeation measurements

In the following, the apparent hydrogen permeability, denoted J_{H_2}, refers to the total amount of hydrogen on the sweep side due to both hydrogen permeation and water splitting.

Figure **3** shows the apparent hydrogen permeability of the cercer membranes with and without Pt-coating as function of inverse temperature in wet 50 % H_2 and with wet and dry sweep gases. It is clear that the apparent hydrogen permeability increases with LWM content at all temperatures and with both wet and dry sweep. Further, the Pt-coating significantly enhances the apparent hydrogen permeability in wet and dry sweep gas with the exception of LWM60-LSC40 with dry sweep (Fig. 3b).

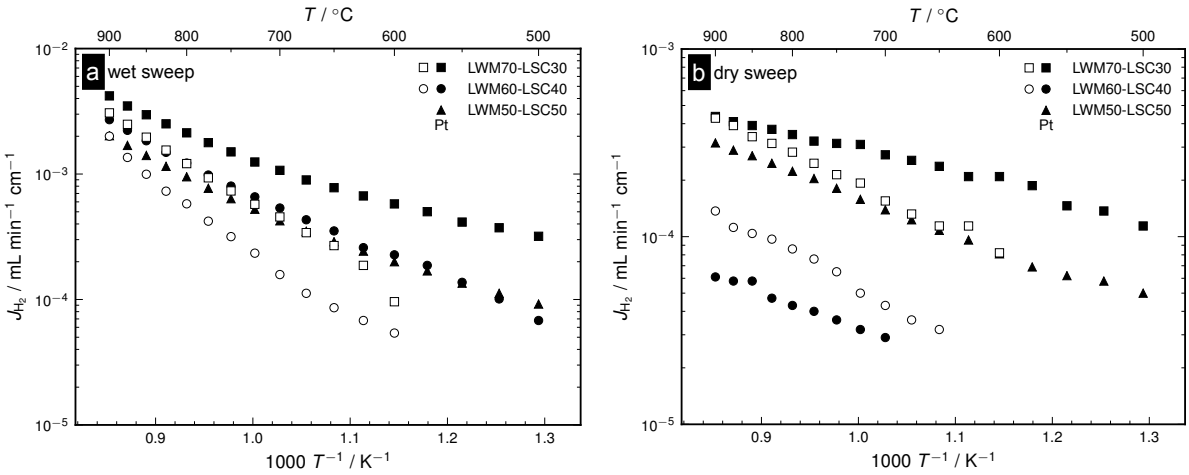

Figure 3: Apparent H_2 permeability of cercer membranes with (filled) and without (open) Pt coating as function of inverse temperature in wet 50 % H_2 as feed and 2.5 % H_2O wetted (a) and dry (b) Ar sweep gas.

In all cases, the enhancement of J_{H_2} by Pt-coating was more pronounced at lower temperatures where surface kinetics are expected to be slower. The activation energies of J_{H_2} in different temperature regimes for the same feed gas as given in Figure 3, and for wet and dry sweep are obtained from the Arrhenius type plot in Figure **4** with the corresponding values listed in Table **1**.

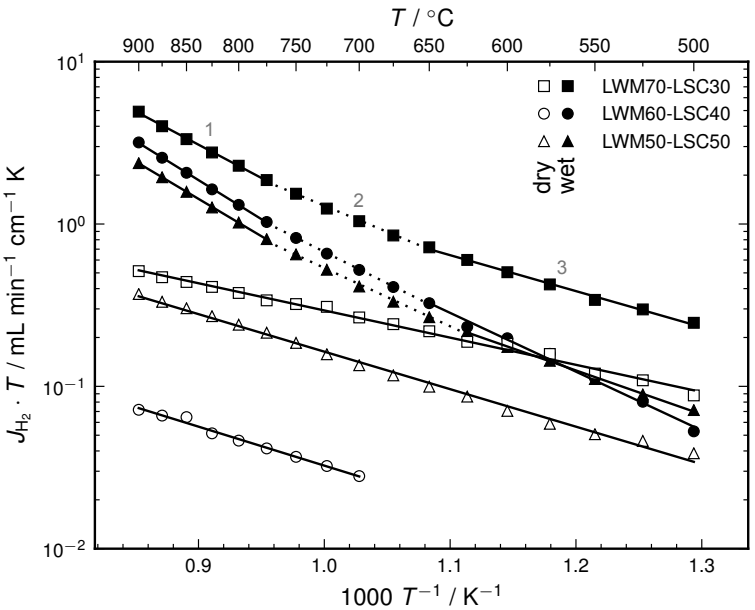

Figure 4: Arrhenius type plot for all Pt-coated samples with wet (filled) and dry (open) sweep gas. The solid and dotted lines represent linear fits and the corresponding activation energies are listed in Table 1 according to the numbered regions.

Table 1: Activation energies of apparent hydrogen permeation in the temperature regions defined in Figure 4 for Pt-coated specimens in wet and dry sweep gas.

Specimen	E_a^1 / kJ mol^{-1}	E_a^2 / kJ mol^{-1}	E_a^3 / kJ mol^{-1}
LWM70-LSC30 wet	79	62	42
LWM60-LSC40 wet	92	74	69
LWM50-LSC50 wet	88	69	52
LWM70-LSC30 dry	32		
LWM60-LSC40 dry	46		
LWM50-LSC50 dry	42		

Figure **5** shows p_{H_2} dependencies of J_{H_2} in wet and dry sweep gas at different temperatures for LWM70-LSC30 with and without Pt-coating. Pt-coating has a minute effect on the functional dependencies of J_{H_2} with respect to p_{H_2} with only a slightly less steep slope with dry sweep; the effect of temperature is much more pronounced.

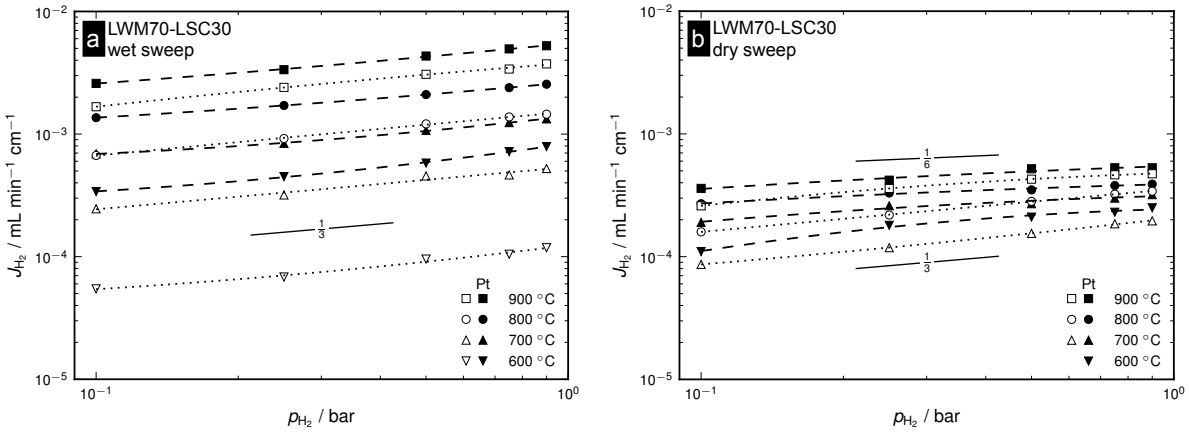

Figure 5: Apparent hydrogen permeability of LWM70-LSC30 with and without Pt-coating as function of feed p_{H_2} between 600 and 900 °C in 2.5 % H_2O wetted (a) and dry (b) sweep gas. The dashed and dotted lines represent second order fitting.

Pt-coating has on the other hand a clear effect on the p_{H_2} dependency for LWM60-LSC40, lowering the functional dependency from approx. $\frac{1}{3}$ to $\frac{1}{4}$ as shown in Figure **6**a. With dry sweep gas, the apparent hydrogen permeability of the Pt-coated sample was too low to obtain reliable data, as indicated by the inset in Figure **6**b.

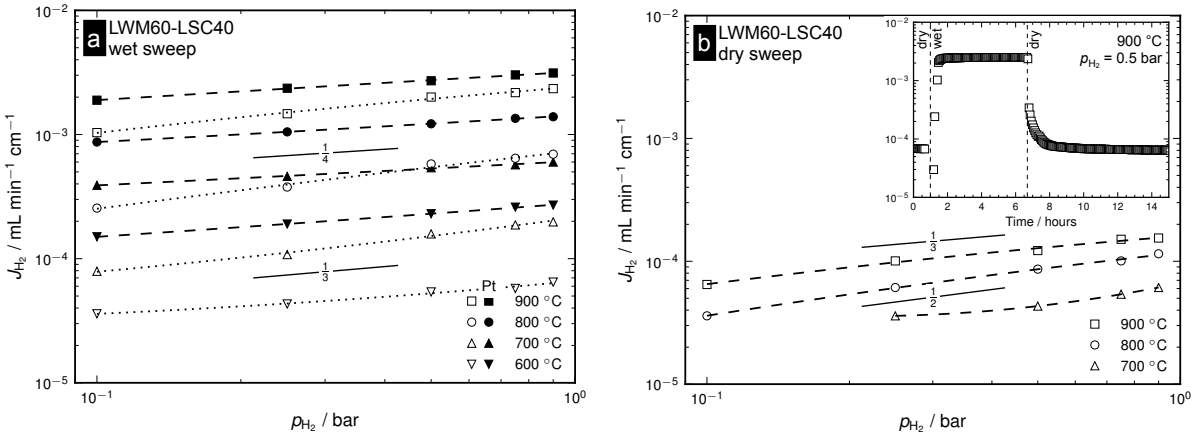

Figure 6: Apparent hydrogen permeability of LWM60-LSC40 with and without Pt-coating as function of feed side p_{H_2} between 600 and 900 °C in 2.5 % H_2O wetted (a) and dry (b) sweep gas. The insert in (b) shows the permeability as function of time with Pt-coating when switching between wet and dry sweep as indicated. The dashed and dotted lines represent second order fitting.

Initial H_2 permeation measurements of a LWM50-LSC50 sample at 1000 °C revealed a continuous decrease in the H_2 permeability from 0.0040 to 0.0017 mL min^{-1} cm^{-1} over 25 hours, mainly in wet 50 % H_2. The sample was cooled in wet 50 % H_2 and XRD analysis revealed formation of additional phases, as reported for LWM by Vøllestad et al.[12] A detailed investigation of the degradation phenomenon including long-term testing will be presented in a forthcoming publication.

4. Discussion

In Figure **7** the apparent hydrogen permeability of the membrane with the highest flux, LWM70-LSC30, is compared with literature data for LWM and LSC. It is evident that the apparent hydrogen permeability LWM70-LSC30 is higher than the individual materials at all temperatures with both wet and dry sweep gas, with an increasing enhancement below approx. 750 °C.

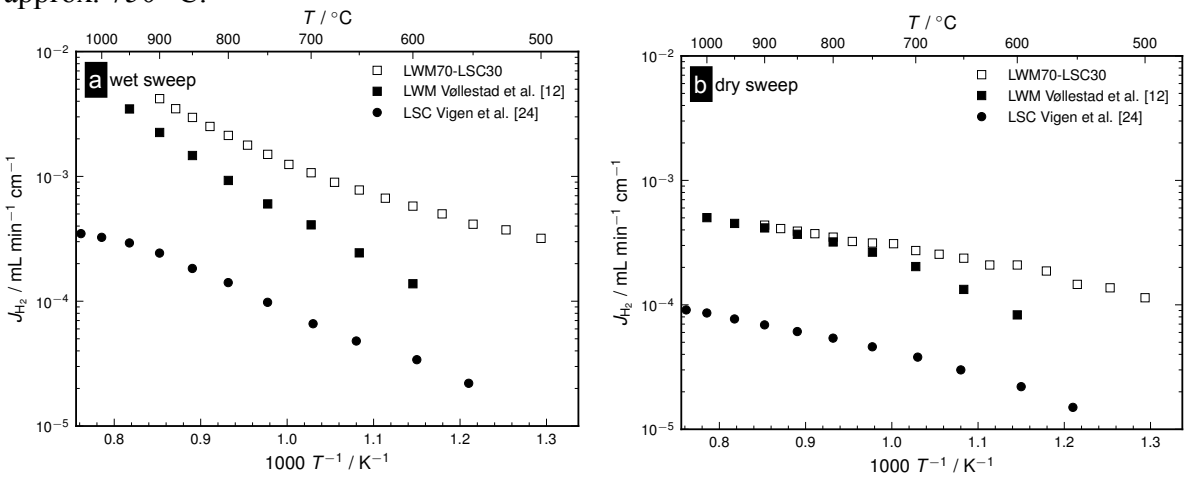

Figure 7: Apparent hydrogen permeability of LWM70-LSC30 membrane (50% H_2 feed) compared to literature values for pure LWM by Vøllestad et al.[12] (97.5% H_2 feed) and LSC by Vigen et al.[24] (10% H_2 feed) with wet (a) and dry (b) sweep gas.

It is reasonable to assert that the ionic transport of the cercer material is governed by the LWM component due to: 1) the apparent hydrogen permeability of LWM is significantly higher than LSC at all temperatures in both wet and dry atmospheres, and 2) LSC is a p-type electronic conductor under all considered conditions and its ambipolar conductivity is therefore limited by ionic species, i.e., LSC cannot significantly contribute to the ionic transport of the cercer material. Accordingly, the relative contributions of H_2 permeation and water splitting to the apparent hydrogen permeability will be determined by the ionic transport of the LWM component. In this respect, the ionic conductivity of LWM transitions from being predominately protonic below approx. 800 °C to be predominated by oxide ions at higher temperatures.[44] Furthermore, the ambipolar conductivity of LWM is electronically limited at temperatures below approx. 750 °C,[44] which corresponds excellently with the temperature regime where the cercer membrane exhibits significantly enhanced hydrogen permeability (Figure **7**).

These considerations can be further supported through evaluation of the activation energies of the apparent hydrogen permeability. The activation energies at high temperatures with wet sweep gas, 79-92 kJ mol^{-1} (E_a^1 in Table **1**), are similar to that reported for pure LWM, 95 kJ mol^{-1}.[12] These values compare well with activation energies of oxide ion transport in non Mo-doped material, 85 and 93 kJ mol^{-1},[31,35] which is consistent with the apparent hydrogen permeability being predominated by water splitting and limited by oxide ion transport under these conditions. H_2 permeation is expected to predominate with dry sweep gas and to be significant at lower temperatures with wet sweep gas, where the activation energies are 32-46 kJ mol^{-1} and 42-69 kJ mol^{-1} (E_a^3 in Table **1**), respectively. These values compare reasonably well to LWM which exhibits an activation energy of 50 kJ mol^{-1} while reaching 40 and 25 kJ mol^{-1} with dry sweep above 800 °C where electronic conductivity is not limiting for feed H_2 concentrations of 10 and 97.5 %, respectively.[12] These activation energies are generally lower than reported values for the enthalpy of mobility of protons, 60 kJ mol^{-1} without Mo-doping[35] and activation energy of proton conductivity 48-61 kJ mol^{-1} for LWM with 0.2-0.4 mol% Mo-doping.[11] The rather large variation in activation energies associated with proton transport indicate a significant dependence on structure and doping, particularly since enthalpies of mobility often are obtained at lower temperatures where ordering and trapping of protons play a significant role.

The apparent H_2 permeability is 2.8 times higher with wet compared to dry sweep gas at 500 °C. This difference may in part be ascribed to a contribution from water splitting with wet sweep although oxide ion conductivity is quite low at this temperature.[44] Moreover, the concentration of protons, and consequently the ambipolar proton electron conductivity and H_2 flux, will be lower at the dry sweep side of the membrane due to dehydration. In this respect, Xing et al.[45] calculated that the overall proton conductivity with wet (2.5% H_2O) compared to dry sweep (5 ppm H_2O) would be higher by a factor of 1.5 within their assumptions for $Gd_{27}W_5O_{55.5-\delta}$.

The highest apparent H_2 permeability was observed for the cercer membrane with 30 wt% (29.3 vol%) LSC, and complete percolation of the electronically conducting LSC phase may not be fully achieved. The hydrogen permeation measurements therefore indicate that a continuous network of electronically conducting LSC is not necessary in order to obtain a significant enhancement in the apparent H_2 permeability. The enhanced apparent H_2 permeability can be attributed to the overall increased electronic conductivity of the cercer material with addition of the higher electronically conducting LSC phase.

The p_{H_2} dependencies of the apparent hydrogen permeability of the cercer materials are in general more shallow than the functional dependencies of up to $\frac{1}{2}$ and 1 observed for LWM and LSC, respectively.[12,24] Considering the significant contribution of many species – protons, oxide ions, electrons and holes – for both phases in the cercer membrane, it is

reasonable that there is not a specific defect situation limiting the apparent H_2 permeability. Furthermore, the clear difference in the p_{H_2} dependencies between uncoated and Pt-coated LWM60-LSC40 with wet sweep (Figure **6**a) may be attributed to the significant surface limitation of LSC.[24] With dry sweep gas (Figure **6**b), the apparent H_2 permeability follows essentially a functional dependency of Log J_{H_2} proportional to $\frac{1}{2}$, which is the theoretical value for bulk H_2 permeation limited by the concentration of protons in an acceptor doped system.[46] Accordingly, the J_{H_2} of LWM60-LSC40 may not be surface limited with dry sweep gas, which complies with the relatively low permeability under these conditions. Furthermore, this also explains the reduced H_2 permeability of LWM60-LSC40 with Pt-coating (Figure **3**b): the Pt-coating reduces the H_2 permeable area of the sample.[47]

Cercer membranes of LWM-LSC show significant promise in comparison with other state-of-the-art ceramic hydrogen membranes. The apparent H_2 permeability of LWM70-LSC30 is 1.1×10^{-3} mL min^{-1} cm^{-1} at 700 °C with wet 50% H_2 feed and wet sweep (2.5% H_2O). This is almost one order of magnitude higher than that reported by Song et al.[10] for $SrCe_{0.95}Eu_{0.05}O_{3-\delta}$, 1.2×10^{-4} mL min^{-1} cm^{-1}, while slightly lower than the 5.5 and 5.9×10^{-3} mL min^{-1} cm^{-1} recently reported by Escolástico et al. for a similar $La_{27}W_5O_{55.5-\delta}$ and LSC based cercer membranes[22] and for Re-substituted lanthanum tungstate, $La_{27.5}W_4ReO_{56.25-\delta}$,[48] respectively. The apparent discrepancy between the measured H_2 permeability between similar cercer membranes may be due to differences in composition, morphology and fabrication procedures, including mixing and sintering temperatures. Optimization of the lanthanum tungstate and cercer systems including surface activation layers should further address the formation of secondary phases and flux degradation.

5. Conclusions

The apparent hydrogen permeability of cercer membranes of $La_{27}W_{3.5}Mo_{1.5}O_{55.5-\delta}$ (LWM) containing 30, 40 and 50 wt% $La_{0.87}Sr_{0.13}CrO_{3-\delta}$ (LSC) were characterized as a function of temperature and feed side p_{H_2} with wet and dry sweep gas. The apparent H_2 permeability was highest for LWM70-LSC30 with both wet and dry sweep gas (2.5 % H_2O), and it was significantly enhanced by the application of a porous Pt-layer, particularly at lower temperatures. It was substantiated that the ionic transport of the cercer membranes is dominated by the LWM component, while LSC contributes with significant p-type electronic conductivity. As such, the advantage of the cercer system becomes more significant at lower temperatures, i.e., 500-750 °C, where electronic conductivity limits the apparent H_2 permeability of pure LWM. Furthermore, water splitting at the sweep side due to oxide ion transport through the membrane predominates the apparent hydrogen permeability at higher temperatures.

The present work demonstrates that cercer membranes are promising for enhancing the ambipolar ionic-electronic conductivity and gas permeability relative to the individual components. The apparent H_2 permeability of LWM70-LSC30 was 1.1×10^{-3} mL min^{-1} cm^{-1} at 700 °C with wet 50% H_2 feed and wet sweep.

Acknowledgements

This publication has been produced with support from the BIGCCS Centre, performed under the Norwegian research program Centres for Environment-friendly Energy Research (FME). The authors acknowledge the following partners for their contributions: ConocoPhillips, Gassco, Shell, Statoil, TOTAL, GDF SUEZ and the Research Council of Norway (193816/S60). The research leading to these results has received funding from the European Union‘s Seventh Framework Programme under Grant Agreement 280765 (BUONAPART-E). The authors wish to acknowledge Protia AS (NO) (subsidiary of CoorsTek, USA) for fruitful discussions.

References

[1] R. Bredesen, K. Jordal, O. Bolland, High-temperature membranes in power generation with CO_2 capture, Chem. Eng. Process. Process Intensif. 43 (2004) 1129–1158.

[2] J.W. Phair, S.P.S. Badwal, Review of proton conductors for hydrogen separation, Ionics. 12 (2006) 103–115.

[3] F. Gallucci, E. Fernandez, P. Corengia, M. van Sint Annaland, Recent advances on membranes and membrane reactors for hydrogen production, Chem. Eng. Sci. 92 (2013) 40–66.

[4] G.Q. Lu, J.C. Diniz da Costa, M. Duke, S. Giessler, R. Socolow, R.H. Williams, et al., Inorganic membranes for hydrogen production and purification: a critical review and perspective., J. Colloid Interface Sci. 314 (2007) 589–603.

[5] J.B. Smith, K.I. Aasen, K. Wilhelmsen, D. Käka, T. Risdal, A. Berglund, et al., Recent development in the HMR pre-combustion gas power cycle, Energy Procedia. 1 (2009) 343–351.

[6] L. Li, R.W. Borry, E. Iglesia, Design and optimization of catalysts and membrane reactors for the non-oxidative conversion of methane, Chem. Eng. Sci. 57 (2002) 4595–4604.

[7] M. Fontaine, T. Norby, Y. Larring, T. Grande, R. Bredesen, Oxygen and Hydrogen Separation Membranes Based on Dense Ceramic Conductors, Membr. Sci. Technol. 13 (2008) 401–458.

[8] S.P. Jiang, S.H. Chan, A review of anode materials development in solid oxide fuel cells, J. Mater. Sci. 39 (2004) 4405–4439.

[9] H. Matsumoto, T. Shimura, T. Higuchi, H. Tanaka, K. Katahira, T. Otake, et al., Protonic-Electronic Mixed Conduction and Hydrogen Permeation in $BaCe_{0.9-x}Y_{0.1}Ru_xO_{3-\alpha}$, J. Electrochem. Soc. 152 (2005) A488.

[10] S. Song, E.D. Wachsman, J. Rhodes, S.E. Dorris, U. Balachandran, Hydrogen permeability of $SrCe_{1-x}M_xO_{3-\delta}$ (x=0.05, M=Eu, Sm), Solid State Ionics. 167 (2004) 99–105.

[11] M. Amsif, A. Magrasó, D. Marrero-López, J.C. Ruiz-Morales, J. Canales-Vázquez, P. Núñes, Mo-Substituted Lanthanum Tungstate A $La_{28-y}W_{4+y}O_{54+\delta}$: Competitive Mixed Electron–Proton Conductor for Gas Separation Membrane Applications, Chem. Mater. 24 (2012) 3868–3877.

[12] E. Vøllestad, C.K. Vigen, A. Magrasó, R. Haugsrud, Hydrogen permeation characteristics of $La_{27}Mo_{1.5}W_{3.5}O_{55.5}$, J. Memb. Sci. 461 (2014) 81–88.

[13] G. Zhang, Interfacial resistances of Ni–BCY mixed-conducting membranes for hydrogen separation, Solid State Ionics. 159 (2003) 121–134.

[14] C. Zuo, T.H. Lee, S.E. Dorris, U. Balachandran, M. Liu, Composite Ni–$Ba(Zr_{0.1}Ce_{0.7}Y_{0.2})O_3$ membrane for hydrogen separation, J. Power Sources. 159 (2006) 1291–1295.

[15] S. Okada, A. Mineshige, T. Kikuchi, M. Kobune, T. Yazawa, Cermet-type hydrogen separation membrane obtained from fine particles of high temperature proton-conductive oxide and palladium, Thin Solid Films. 515 (2007) 7342–7346.

[16] J. Hardy, E. Thomsen, N. Canfield, J. Crum, K. Scottweil, L. Pederson, Development of passive hydrogen separation membranes made from Co-synthesized nanoscale cermet powders, Int. J. Hydrogen Energy. 32 (2007) 3631–3639.

[17] S. Fang, L. Bi, L. Yan, W. Sun, CO_2 Resistant Hydrogen Permeation Membranes Based on Doped Ceria and Nickel, J. Phys. Chem. C. (2010) 10986–10991.

[18] A. Unemoto, A. Kaimai, K. Sato, K. Yashiro, H. Matsumoto, J. Mizusaki, et al., Hydrogen permeability and electrical properties in oxide composites, Solid State Ionics. 178 (2008) 1663–1667.

[19] W. Xing, G.E. Syvertsen, T. Grande, Z. Li, R. Haugsrud, Hydrogen permeation, transport properties and microstructure of Ca-doped $LaNbO_4$ and $LaNb_3O_9$ composites, J. Memb. Sci. 415-416 (2012) 878–885.

[20] J.S. Fish, S. Ricote, F. Lenrick, L.R. Wallenberg, T.C. Holgate, R. O'Hayre, et al., Synthesis by spark plasma sintering of a novel protonic/electronic conductor composite: $BaCe_{0.2}Zr_{0.7}Y_{0.1}O_{3-\delta}$ /$Sr_{0.95}Ti_{0.9}Nb_{0.1}O_{3-\delta}$ (BCZY27/STN95), J. Mater. Sci. 48 (2013) 6177–6185.

[21] J.M. Serra, S. Escolástico, Patent, PCT/EP2014/060708, 2014.

[22] S. Escolastico, S. Cecilia, C. Kjølseth, J.M. Serra, Outstanding hydrogen permeation through CO_2-stable dual phase ceramic membranes, Energy Environ. Sci. (2014).

[23] Y. Larring, C. Vigen, F. Ahouanto, M.-L. Fontaine, T. Peters, J.B. Smith, et al., Investigation of $La_{1-x}Sr_xCrO_{3-\delta}$ (x ~ 0.1) as Membrane for Hydrogen Production, Membranes. 2 (2012) 665–686.

[24] C.K. Vigen, R. Haugsrud, Hydrogen flux in $La_{0.87}Sr_{0.13}CrO_{3-\delta}$, J. Memb. Sci. 468 (2014) 317–323.

[25] R. Haugsrud, Defects and transport properties in Ln_6WO_{12} (Ln=La, Nd, Gd, Er), Solid State Ionics. 178 (2007) 555–560.

[26] R. Haugsrud, H. Fjeld, K.R. Haug, T. Norby, Mixed Ionic and Electronic Conductivity of Undoped and Acceptor-Doped Er_6WO_{12}, J. Electrochem. Soc. 154 (2007) B77.

[27] R. Haugsrud, C. Kjølseth, Effects of protons and acceptor substitution on the electrical conductivity of La_6WO_{12}, J. Phys. Chem. Solids. 69 (2008) 1758–1765.

[28] S. Escolástico, V.B. Vert, J.M. Serra, Preparation and Characterization of Nanocrystalline Mixed Proton−Electronic Conducting Materials Based on the System Ln_6WO_{12}, Chem. Mater. 21 (2009) 3079–3089.

[29] A. Magrasó, C. Frontera, D. Marrero-López, P. Núñez, New crystal structure and characterization of lanthanum tungstate "La_6WO_{12}" prepared by freeze-drying synthesis., Dalt. Trans. (2009) 10273–83.

[30] S. Escolástico, C. Solís, J.M. Serra, Hydrogen separation and stability study of ceramic membranes based on the system Nd_5LnWO_{12}, Int. J. Hydrogen Energy. 36 (2011) 11946–11954.

[31] C. Solís, S. Escolastico, R. Haugsrud, J.M. Serra, Characterization of Transport Properties under Oxidizing Conditions: A Conductivity Relaxation Study, J. Phys. Chem. C. (2011) 11124–11131.

[32] J. Seeger, M.E. Ivanova, W. a Meulenberg, D. Sebold, D. Stöver, T. Scherb, et al., Synthesis and characterization of nonsubstituted and substituted proton-conducting $La_{6-x}WO_{12-y}$., Inorg. Chem. 52 (2013) 10375–86.

[33] S. Escolástico, C. Solís, T. Scherb, G. Schumacher, J.M. Serra, Hydrogen separation in $La_{5.5}WO_{11.25-\delta}$ membranes, J. Memb. Sci. 444 (2013) 276–284.

[34] A. Magrasó, J.M. Polfus, C. Frontera, J. Canales-Vázquez, L.-E. Kalland, C.H. Hervoches, et al., Complete structural model for lanthanum tungstate: a chemically stable high temperature proton conductor by means of intrinsic defects, J. Mater. Chem. 22 (2012) 1762.

[35] S. Erdal, L.-E. Kalland, R. Hancke, J. Polfus, R. Haugsrud, T. Norby, et al., Defect structure and its nomenclature for mixed conducting lanthanum tungstates $La_{28-x}W_{4+x}O_{54+3x/2}$, Int. J. Hydrogen Energy. 37 (2012) 8051–8055.

[36] N. Sakai, T. Kawada, H. Yokokawa, Sinterability and electrical conductivity of calcium-doped lanthanum chromites, J. Mater. Sci. 25 (1990) 4531–4534.

[37] P. Devi, M. Subba Rao, Preparation, Structure, and Properties of Strontium-Doped Lanthanum Chromites: $La_{1-x}Sr_xCrO_3$, J. Solid State Chem. 98 (1992) 237–244.

[38] B.A. van Hassel, T. Kawada, N. Sakai, H. Yokokawa, M. Dokiya, Oxygen permeation modelling of $La_{1-y}Ca_yCrO_{3-\delta}$, Solid State Ionics. 66 (1993) 41–47.

[39] T. Kawada, T. Horita, N. Sakai, H. Yokokawa, M. Dokiya, Experimental determination of oxygen permeation flux through bulk and grain boundary of $La_{0.7}Ca_{0.3}CrO_3$, Solid State Ionics. 79 (1995) 201–207.

[40] S. Julsrud, B.E. Vigeland, Solid multicomponent mixed proton and electron conducting membrane, EP Patent 1448293, 2007.

[41] M. Mori, Y. Hiei, N. Sammes, Sintering behavior and mechanism of Sr-doped lanthanum chromites with A site excess composition in air, Solid State Ionics. 123 (1999) 103–111.

[42] S. Simner, J. Hardy, J. Stevenson, T. Armstrong, Sintering of lanthanum chromite using strontium vanadate, Solid State Ionics. 128 (2000) 53–63.

[43] M. Mori, T. Yamamoto, T. Ichikawa, Y. Takeda, Dense sintered conditions and sintering mechanisms for alkaline earth metal (Mg, Ca and Sr)-doped $LaCrO_3$ perovskites under reducing atmosphere, Solid State Ionics. 148 (2002) 93–101.

[44] A. Magrasó, Transport number measurements and fuel cell testing of undoped and Mo-substituted lanthanum tungstate, J. Power Sources. 240 (2013) 583–588.

[45] W. Xing, P. Rauwel, C.H. Hervoches, Z. Li, R. Haugsrud, Structure and transport properties in un-doped and acceptor-doped gadolinium tungstates, Solid State Ionics. 261 (2014) 87–94.

[46] T. Norby, R. Haugsrud, Dense Ceramic Membranes for Hydrogen Separation, in Membranes for Energy Conversion, Wiley-ECH Verlag Gmbh & Co KGaA, 2008.

[47] N.W. Ockwig, T.M. Nenoff, Membranes for hydrogen separation., Chem. Rev. 107 (2007) 4078–110.

[48] S. Escolastico, J. Seeger, S. Roitsch, M. Ivanova, W. a Meulenberg, J.M. Serra, Enhanced H2 separation through mixed proton-electron conducting membranes based on $La_{5.5}W_{0.8}M_{0.2}O_{11.25-\delta}$., ChemSusChem. 6 (2013) 1523–32.